A Model for Volume Change Dependency of Water Retention Curve

A.Y. Pasha, A. Khoshghalb & N. Khalili
School of Civil and Environmental Engineering, University of New South Wales, Sydney, Australia

ABSTRACT: A model for the evaluation of the void ratio dependency of Water Retention Curve (WRC) in deformable porous media is presented. Models currently available in the literature for this purpose are primarily empirical in nature and rely on extensive laboratory testing for parameter identification. The approach proposed in this paper requires no additional parameters and enables quantification of the dependency of WRC on void ratio solely based on the form of WRC at the reference void ratio. Particular attention is given to the effect of hydraulic hysteresis on the evolution process, an aspect rarely addressed in the literature. Good agreement is obtained between model predictions and experimental data in all the cases considered.

1 INTRODUCTION

Commonly presented as a plot of water content or degree of saturation versus the logarithm of matric suction, Water Retention Curve (WRC) describes the water retention capacity of a soil at any given suction. It enters the constitutive relations of the soil, providing a platform for the coupling of air and water constituents within the system at a macroscopic level (e.g. see Khalili et al. 2000; Vaunat et al. 2000; Gallipoli et al. 2003b; Wheeler et al. 2003; Khalili et al. 2008; Khoshghalb and Khalili 2013). In addition, it is extensively used for quantifying unsaturated soil properties such as water and air relative permeabilities (Corey et al. 1956; Mualem 1976; Lenhard and Parker 1987), shear strength properties (Fredlund et al. 1978; Vanapalli et al. 1996), effective stress parameter (Khalili and Khabbaz 1998; Khalili et al. 2004; Lu and Likos 2006) and deformation and swelling characteristic (Matyas and Radhakrishna 1968; Biarez et al. 1987).

Numerous relationships have been presented in the literature for the mathematical representation of WRC (e.g. Brooks and Corey 1964; van Genuchten 1980; Fredlund and Xing 1994). However, a vast majority has been for non-deformable soils ignoring the impact of volume change on WRC (Pasha et al., 2015). The soil structural changes directly affect soil water movement by altering the hydraulic properties that are commonly described by WRC.

The main contributions to the evolution of WRC with volume change have been due to Wheeler et al. (2003), Gallipoli et al. (2003a), Nuth and Laloui (2008), Tarantino (2009), Romero et al. (2011), Gallipoli (2012), and Zhou et al. (2012). The available models are, however, often empirical in nature and mainly rely on fitting parameters. Excessive experimental time and cost related to the quantification of the embedded parameters in the existing models is a major issue in the process of the application of such models in the geotechnical engineering practice. More importantly, the influence of volumetric deformations on the evolution of the scanning path of WRC, i.e. the hysteresis effect, has been rarely investigated. This is despite the fact that essentially in the majority of cases, either in laboratory investigations on unsaturated soils or in real-life, the loading/unloading of soils are being done on the scanning path of WRC.

In this paper, an approach for the evolution of WRC with void ratio within the theoretical framework of Khalili et al. (2008) is presented. The model proposed is an extension of the work by Mašín (2010) and includes the effects of hydraulic hysteresis and a change in void ratio on both branches of main wetting and drying curves, as well as transition from wetting to drying and vice versa. Particular attention is given to the scanning behavior of the soil and the dependency of pore size distribution to void ratio. The approach proposed is general in nature, requires no additional parameters, and allows prediction of the shift in WRC with volume change entirely based on the form of WRC at a reference void ratio. The applicability of the model to an extensive array of experimental data is demonstrated.

2 PRELIMINARIES

Following the fundamental contribution of Khalili et al. (2008), the water volumetric strain (dV_w/V where V_w and V are water volume and total volume of soil, respectively) is related to the total volumetric strain ($d\varepsilon_v = dV/V = dV_v/V$ where V_v is the volume of voids) in incremental from, as

$$-\frac{dV_w}{V} = \psi d\varepsilon_v + ads \tag{1}$$

where a is the constitutive coefficient relating water retention at constant volume to a change in suction, and ψ can be calculated from

$$\psi = \frac{\partial(\chi s)}{\partial s} = \left(1-\frac{\partial \ln \chi}{\partial \ln s}\right)\chi \tag{2}$$

in which χ is the effective stress parameter in total form which describes the contribution of suction to the effective stress of the soil solid skeleton. Note that in (2), $\partial ln\chi/\partial lns$ is taken as positive when χ decreases with an increase in suction. Earlier definitions of the effective stress parameter assumed direct correlation with the degree of saturation, $\chi = S_r$ (Bishop and Blight, 1963). However, it was shown in many recent works (e.g., Hassanizadeh and Gray, 1990; Houlsby, 1997) that only when the work of air-water interface is ignored, the effective stress parameter may be taken as the degree of saturation. Based on back-calculation of unsaturated shear test data for many soil types, Khalili and Khabbaz (1998) proposed an equation for the effective stress parameter. In this work, the hysteretic effective stress parameter, χ, is quantified as follows:

For main wetting and drying paths

$$\chi = \begin{cases} 1 & for \quad s < s_e \\ \left(\frac{s_e}{s}\right)^{\Omega} & for \quad s \geq s_e \end{cases} \tag{3-1}$$

For drying path reversals

$$\chi = \left(\frac{s_{ae}}{s_{rd}}\right)^{\Omega}\left(\frac{s_{rd}}{s}\right)^{\zeta} \;;\; \left(\frac{s_{ex}}{s_{ae}}\right)^{\frac{\Omega}{\Omega-\zeta}} s_{rd} \leq s \leq s_{rd} \tag{3-2}$$

For wetting path reversal

$$\chi = \left(\frac{s_{ex}}{s_{rw}}\right)^{\Omega}\left(\frac{s_{rw}}{s}\right)^{\zeta} \;;\; s_{rw} \leq s \leq \left(\frac{s_{ae}}{s_{ex}}\right)^{\frac{\Omega}{\Omega-\zeta}} s_{rw} \tag{3-3}$$

where the air entry, s_{ae}, and air expulsion, s_{ex}, values denote the points of transition from saturation to unsaturation and vice versa along the main drying and main wetting paths, respectively. Ω is the material parameter, with the best fit value of 0.55, ζ is the slope of the transition path between the main drying and wetting paths in a lnχ~ln$s$ plane. s_{rd} and s_{rw} are the points of suction reversal on the main drying and main wetting paths, respectively. A schematic representation of (3) is shown in Figure 1.

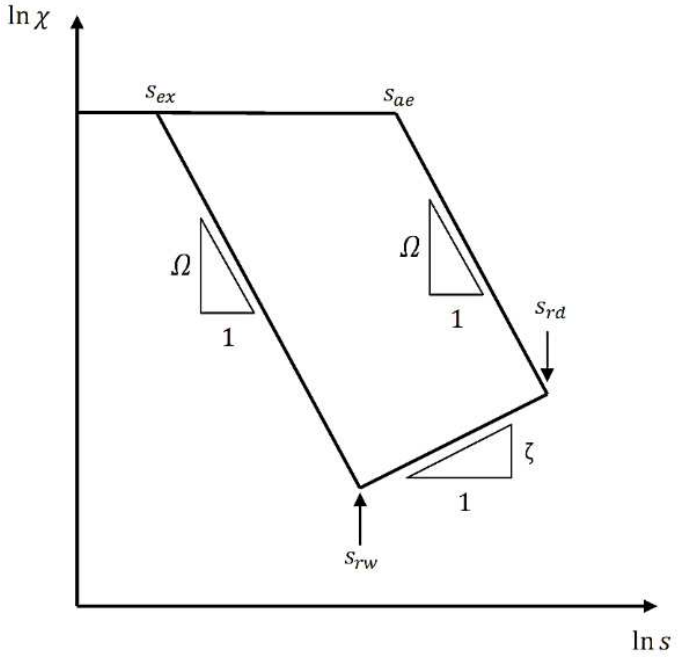

Figure 1. Effective stress parameter versus suction

The effective degree of saturation can also be defined based the model originally proposed by Brooks and Corey (1964) to include hydralic hystersis, as follows:

For main wetting and drying paths

$$S_{eff} = \begin{cases} 1 & for \quad s < s_e \\ \left(\frac{s_e}{s}\right)^{\lambda_p} & for \quad s \geq s_e \end{cases} \tag{4-1}$$

For drying path reversals

$$S_{eff} = \left(\frac{s_{ae}}{s_{rd}}\right)^{\lambda_p}\left(\frac{s_{rd}}{s}\right)^{\xi} \;;\; \left(\frac{s_{ex}}{s_{ae}}\right)^{\frac{\lambda_p}{\lambda_p-\xi}} s_{rd} \leq s \leq s_{rd} \tag{4-2}$$

For wetting path reversal

$$S_{eff} = \left(\frac{s_{ex}}{s_{rw}}\right)^{\lambda_p}\left(\frac{s_{rw}}{s}\right)^{\xi} \;;\; s_{rw} \leq s \leq \left(\frac{s_{ae}}{s_{ex}}\right)^{\frac{\lambda_p}{\lambda_p-\xi}} s_{rw} \tag{4-3}$$

where $S_{eff} = (S_r - S_{res})/(1 - S_{res})$ is the effective degree of saturation, λ_p is the pore size distribution index or the slope of the WRC in a $\ln S_{eff} \sim \ln s$ plane, and ξ is the slope of the scanning path between the main drying and wetting paths in a $\ln S_{eff} \sim \ln s$ plane.

3 MODEL DEVELOPMENT

The definition of the degree of saturation, S_r, and the assumption that solids are incompressible, yields,

$$\frac{dV_w}{V} = S_r\frac{dV_v}{V} + ndS_r = -S_r d\varepsilon_v + ndS_r \tag{5}$$

in which n is the porosity. It is noted that,

$$dS_r = \frac{\partial S_r}{\partial s}ds + \frac{\partial S_r}{\partial \varepsilon_v}d\varepsilon_v \tag{6}$$

Substituting for dS_r from (6) in (5) results in,

$$\frac{dV_w}{V} = -\left(S_r - n\frac{\partial S_r}{\partial \varepsilon_v}\right)d\varepsilon_v + n\frac{\partial S_r}{\partial s}ds \quad (7)$$

and comparing (7) with (1) yields,

$$\psi = S_r - n\frac{\partial S_r}{\partial \varepsilon_v} \quad (8\text{-}1)$$

$$a = -n\frac{\partial S_r}{\partial s} \quad (8\text{-}2)$$

which describe a and ψ in terms of n, $\partial S_r/\partial s$ and the evolution of WRC with volumetric strain, $\partial S_r/\partial \varepsilon_v$. Noting $dn = (n-1)d\varepsilon_v$, (8-1) is rearranged to

$$dS_r = (\psi - S_r)\frac{de}{e} \quad (9)$$

where $e = n/(1-n)$ is the void ratio. Now, combining (3), (4) and (9), an expression for the evolved (updated) main drying ($s_e = s_{ae}$) and wetting ($s_e = s_{ex}$) curves; i.e. due to an infinitesimal increment in the void ratio, is obtained as

$$S^*_{eff} = S_{eff} + dS_{eff} = \left(\frac{s_e}{s}\right)^{\lambda_p} + \frac{\left((1-\Omega)\left(\frac{s_e}{s}\right)^{\Omega} - (1-S_{res})\left(\frac{s_e}{s}\right)^{\lambda_p} - S_{res}\right)}{e(1-S_{res})}de \quad (10)$$

The updated scanning curve is in turn obtained in a similar manner as

$$S^*_{eff} = S_{eff} + dS_{eff} = \left(\frac{s_e}{s_r}\right)^{\lambda_p}\left(\frac{s_r}{s}\right)^{\xi} + \frac{\left((1-\zeta)\left(\frac{s_e}{s_r}\right)^{\Omega}\left(\frac{s_r}{s}\right)^{\zeta} - (1-S_{res})\left(\frac{s_e}{s_r}\right)^{\lambda_p}\left(\frac{s_r}{s}\right)^{\xi} - S_{res}\right)}{e(1-S_{res})}de \quad (11)$$

s_r in (11) refers to the point of suction reversal on the main drying and wetting curves, with $s_r = s_{rd}$ representing the reversal from the main drying curve and $s_r = s_{rw}$ capturing the reversal from the main wetting curve. Notice that all updated parameters are denoted by an asterisk.

To obtain the updated air entry/air expulsion value (s^*_e), (10) is considered at its limit of transition from saturation to unsaturation, where S^*_{eff}=1, and $s = s^*_e$, yielding

$$\frac{(1-\Omega)de}{e(1-S_{res})}\left(\frac{s_e}{s^*_e}\right)^{\Omega} + \left(1-\frac{de}{e}\right)\left(\frac{s_e}{s^*_e}\right)^{\lambda_{psu}} - \left(1 + \frac{S_{res}de}{e(1-S_{res})}\right) = 0 \quad (12)$$

where λ_{psu} is the pore size distribution index at the point of transition from saturation to unsaturation, and s^*_e is the air entry value corresponding to the updated void ratio $e + de$. For small increments of void ratio, an approximate solution can be found for s^*_e using Taylor's series (Pasha et al. 2017), yielding the following expression for the evolution of air entry (or air expulsion) value with void ratio,

$$s^*_e = s_e\left(1 + \frac{\Omega}{(1-S_{res})}\frac{de}{e}\right)^{-1/\lambda_{psu}} \quad (13)$$

which results in the following estimation for the change in the air entry/expulsion value due to a small increment in void ratio,

$$\frac{ds_e}{s_e} = -\frac{\Omega}{(1-S_{res})\lambda_{psu}}\frac{de}{e} \quad (14)$$

This is the same as the expression previously derived by Mašín (2010) for the evolution of the air entry value with void ratio.

To capture the dependency of λ_p to void ratio, it is first noted that for the main drying and wetting paths, the variation of the degree of saturation with e can be expressed as,

$$\frac{\partial S_r}{\partial e} = \frac{\partial S_r}{\partial s_e}\frac{\partial s_e}{\partial e} + \frac{\partial S_r}{\partial \lambda_p}\frac{\partial \lambda_p}{\partial e} \quad (15)$$

Calculating the partial derivatives of S_r with respect to s_e and λ_p using (4-1) and substituting from (9) and (14) in (15), the variation of λ_p with respect to e can be obtained,

$$\frac{\partial \lambda_p}{\partial e} = \frac{\psi - S_r + \Omega S_{eff}\frac{\lambda_p}{\lambda_{psu}}}{(1-S_{res})S_{eff}lnS_{eff}}\frac{\lambda_p}{e} \quad (16)$$

which can be used to calculate the updated pore size distribution index, λ^*_p. Notice that the λ^*_p is obtained from a secant approach, i.e. from the point of air entry/expulsion to the point of interest on the main path of WRC. From (16), the limiting value of λ^*_p=λ^*_{psu} at $s = s^*_e$, is obtained as, (Pasha et al. 2017)

$$\lambda^*_{psu} = \lambda_{psu}\left[1 + \left(\frac{(1-\Omega+\lambda_{psu})\Omega}{(1-S_{res})\lambda_{psu}} - 1\right)\frac{de}{e}\right] \quad (17)$$

It is noted that (16) shows some dependency of $\partial\lambda_p/\partial e$ to suction, s. However, such dependency is very slight and may be omitted with little influence on the evolution calculations of WRC with void ratio (Mašín 2010). To remove dependency of $\partial\lambda_p/\partial e$ to suction (16) is linearised between points $[s_e/s = 1\ ,\ S_{eff} = 1\ ]$ and $[s_e/s = (0.5)^{1/\lambda_p},\ S_{eff} = 0.5]$, leading to

$$\lambda^*_p = \lambda_p\left[1 - \frac{3\left((1-\Omega)\left(2^{(1-\Omega/\lambda_p)}-1\right) - Sres\right)}{2(1-S_{res})}\frac{de}{e}\right] \quad (18)$$

If volume change occurs when the hydraulic state is on the scanning curve, updated slope of the scanning curve (ξ^*) must also be calculated. This is obtained from the slope of the tangent to (11) at the point of interest as (Pasha et al., 2017)

$$\xi^* = \xi\left[1 + \frac{(1-\zeta)(\zeta-\xi)}{\xi}S_{eff,r}^{\frac{\Omega}{\lambda_p}-1}\frac{de}{e}\right] = \xi\left[1 + \frac{(1-\zeta)(\zeta-\xi)}{\xi}\left(\frac{s_e}{s_r}\right)^{\Omega-\lambda_p}\frac{de}{e}\right] \quad (19)$$

where $S_{eff,r}$ is the effective degree of saturation at the point of suction reversal. The updated s_r is in

turn obtained from the intersection of (19) with the updated main wetting and drying curves as

$$s_r^* = \left(\frac{(s_e^*)^{\lambda_p^*}}{s^{\xi^*} S_{eff}^*}\right)^{\frac{1}{(\lambda_p^* - \xi^*)}} \quad (20)$$

where S_{eff}^* is the updated effective degree of saturation at the point of interest on the scanning curve calculated from (11). Comparing the suction at the point of interest, s, to s_r^* from (20) at each step of the calculation determines whether the soil hydraulic state is on the scanning path or it has moved to the main path due to the change in the void ratio.

Finally, satisfying the constraint that the points of transition from drying to wetting and vice versa must coincide in both $\ln S_{eff} \sim \ln s$ and $\ln \chi \sim \ln s$ planes, yields

$$\zeta^* = \Omega \xi^* \left(\lambda_{pd}^* + \frac{\left(\lambda_{pw}^* - \lambda_{pd}^*\right) ln\left(\frac{s_{ex}^*}{s_{rw}^*}\right)}{ln\left(\frac{s_{ex}^*}{s_{rw}^*}\right) + ln\left(\frac{s_{rd}^*}{s_{ae}^*}\right)} \right)^{-1} \quad (21)$$

4 MODEL PREDICTIONS AND COMPARISON WITH EXPERIMENTAL RESULTS

In the following, the proposed model is verified using datasets from the literature. Model predictions are compared with experimental data for a range of void ratios and hydraulic states. Two examples are presented: one for the evolution of WRC with void ratio, and one for the variation of the degree of saturation with void ratio at constant suction.

4.1 *Evolution of main path of WRC with void ratio: data on compacted till*

Vanapalli et al. (1999) derived laboratory WRCs of a sandy clay till which contained 8% sand, 41% silt, and 51% clay. The liquid and plastic limits of the soil were reported as 75.5% and 24.9%, respectively. The samples were compressed in conventional odoemeter apparatus under different pressures in order to gain different initial densities prior to WRC tests. The WRCs obtained for these samples in drying path are replotted in Figure 2. The WRC at the most compact state, i.e. $e = 0.444$ was selected as the reference WRC leading to the following model parameters: $s_{e0} = 90\ kPa$; $\lambda_{p0} = 0.12$; $S_{res} = 0.1$; $\Omega = 0.55$; $e_0 = 0.444$. The WRCs predicted at the rest of the void ratios are also plotted in Figure 2. As can be seen from this figure, the predicted water retention behavior at various volumetric states agrees well with the experimental observations.

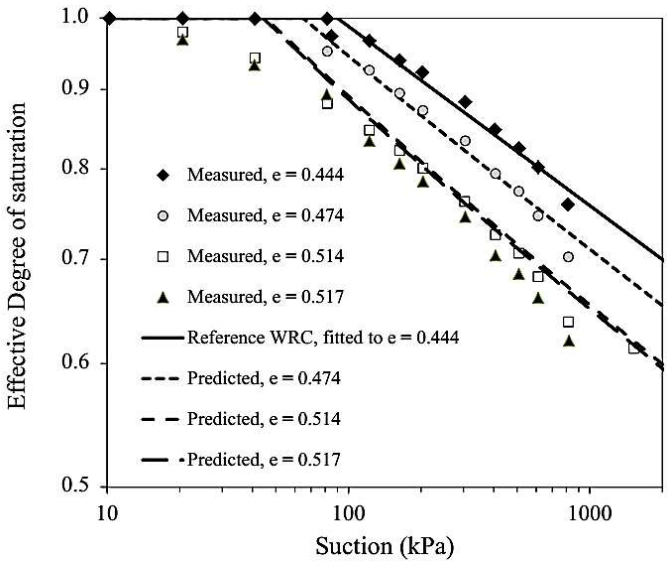

Figure 2. Measured and predicted evolution of the main drying path of WRC with void ratio for compacted till – data after Vanapalli (1999)

4.2 *Variation of degree of saturation at constant-suction loading tests: data on Pearl clay (kaolin)*

Sun et al. (2007) reported results of a series of deviatoric and compression triaxial tests at different constant suctions on unsaturated samples of compacted Pearl clay. The soil consisted of 50% silt and 50% clay (mainly kaolin) with a liquid limit of 49% and a plasticity index of 22%. The specimens were prepared by compaction in a mould at a water content of about 26%, with the after-compaction suctions varying from 100 kPa to 150 kPa. The triaxial tests were performed for a range of isotropic compression and deviatoric loading at different values of constant suction (98, 147, 196, and 245 kPa) as shown in Figure 3.

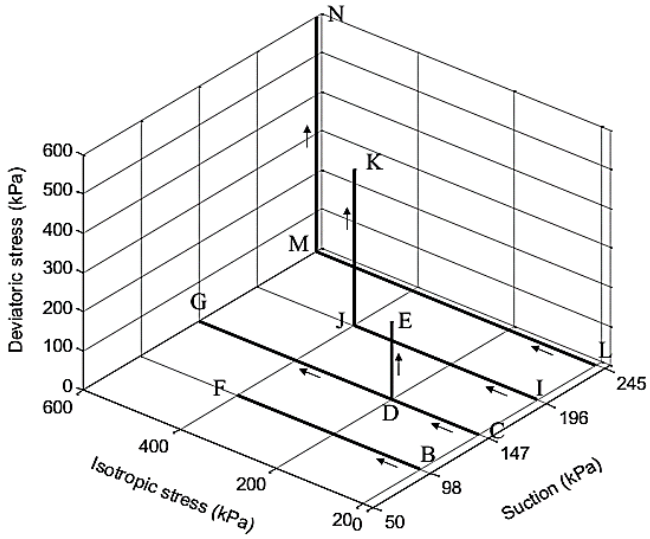

Figure 3. Stress paths for the constant suction loading tests on non-expansive clay (after Sun et al. 2007)

The main wetting curve of the WRC for the above soil obtained at a reference void ratio of 1.299 is illustrated in Figure 4. The input parameters used in the model for the stress paths shown in Figure 3 are: $s_{e0} = 15\,kPa$; $\lambda_{p0} = 0.34$; $\xi_0 = 0.08$; $S_{res} = 0.1$; $\Omega = 0.55$; $\zeta = 0.0$; $e_0 = 1.299$.

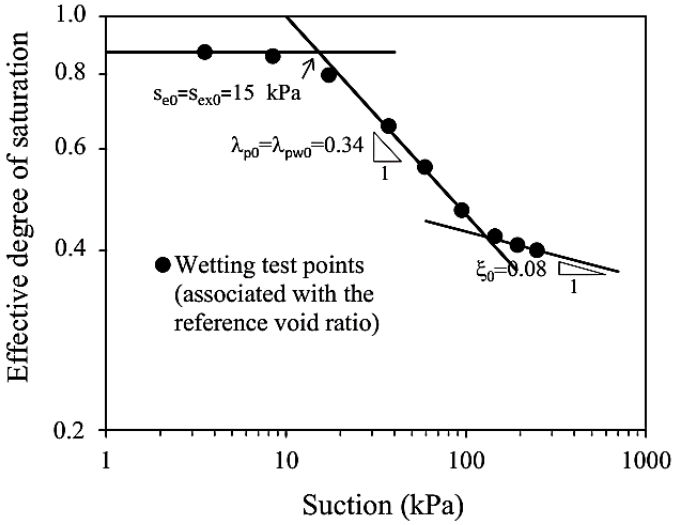

Figure 4. Measured WRC (wetting path) and the calibrated parameters (Data after Sun et al. 2007)

The initial hydraulic state at the start of loading was considered to be scanning drying for path LMN, scanning wetting for paths CDG and IJK, and main wetting for paths CDE and BF. These were ascertained from the target suction and the degree of saturation at the start of each test in comparison with the wetting WRC adjusted for the void ratio at the start of each test.

For all five loading paths, the simulation was performed using the same set of parameters. The results are presented in Figure 5. Model predictions, for path LMN, show that a decrease in the void ratio, causes the soil hydraulic state to change from scanning drying to scanning wetting up to the void ratio of 1.045. The hydraulic state then changes to the main wetting beyond this point until the end of the test. Similar behavior is also observed for paths IJK and CDG. The predicted curves in Figure 5 show that the transition from the scanning wetting to main wetting path occurred at the void ratios of 1.095 and 1.020 for paths IJK and CDG, respectively, which coincide with a slight increase in the rate of change in the degree of saturation with void ratio. The tests with paths CDE and BF continually remain on the main wetting. Figure 5 shows that the proposed model has captured the variation of the degree of saturation with volume remarkably well for volumetric deformations in both isotropic and deviatoric loading paths.

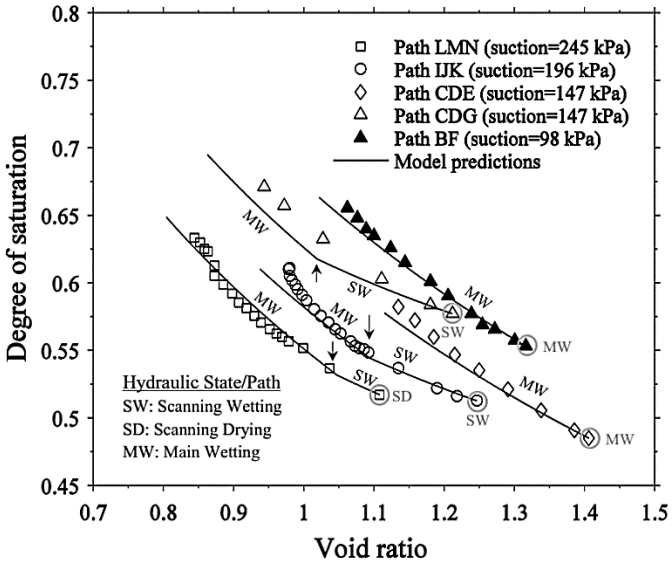

Figure 5. Measured and predicted variation of degree of saturation with void ratio at constant suction isotropic and deviatoric loading paths on non-expansive clay – data after Sun et al. (2007). Arrows show the predicted points of transition from scanning to main wetting path

5 CONCLUSIONS

A model is presented for predicting the volume change dependency of WRC. Unlike previous models of WRC presented in the literature, the proposed model captures the volume change dependency of the WRC without introducing additional soil parameters. The full WRC hysteretic loop is considered enabling the model to capture changes in the degree of saturation in unsaturated soils under constant suction, subjected to mechanical contraction/dilation paths. By constantly updating the WRC with void ratio and identifying new sample hydraulic states, the model is able to predict the complete hydraulic path followed by a soil during mechanical loading. The proposed model is validated against two sets of experimental data from the literature. Remarkable agreement is observed between the model simulations and the experimental data showing that the proposed model can effectively capture the volume change effect on WRC.

6 REFERENCES

Biarez, J., Fleureau, J.M., Zerhouni, M.I., and Soepandji, B.S. 1987. Variations de volume des sols argileux lors de cycles de drainage-humidification. *Revue Francaise de Géotechnique* 41: 63-72.

Bishop, A.W. & Blight, G. 1963. Some aspects of effective stress in saturated and partly saturated soils. *Géotechnique* 13(3): 177-197.

Brooks, R.H.& Corey, A.T. 1964. Hydraulic properties of porous media. *Hydrology Papers*, Colorado State University (March).

Corey, A.T., Rathjens, C.H., Henderson, J.H. & Wyllie, M.R.J. 1956. Three-Phase Relative Permeability. *Transactions of*

the American Institute of Mining and Metallurgical Engineers 207(12): 349-351.

Fredlund, D., Morgenstern, N. & Widger, R. 1978. The shear strength of unsaturated soils. *Canadian Geotechnical Journal* 15(3): 313-321.

Fredlund, D.G. & Xing, A. 1994. Equations for the soil-water characteristic curve. *Canadian Geotechnical Journal* 31(4): 521-532.

Gallipoli, D. 2012. A hysteretic soil-water retention model accounting for cyclic variations of suction and void ratio. *Géotechnique* 62(7): 605-616.

Gallipoli, D., Wheeler, S.J. & Karstunen, M. 2003. Modelling the variation of degree of saturation in a deformable unsaturated soil. *Géotechnique* 53(1): 105-112.

Gallipoli, D., Gens, A., Sharma, R. & Vaunat, J. 2003. An elasto-plastic model for unsaturated soil incorporating the effects of suction and degree of saturation on mechanical behaviour. *Géotechnique* 53(1): 123-135.

Hassanizadeh, S.M. & Gray, W.G. 1990. Mechanics and thermodynamics of multiphase flow in porous media including interphase boundaries. *Advances in Water Resources* 13(4): 169-186.

Houlsby, G.T. 1997. The work input to an unsaturated granular material. *Géotechnique* 47(1): 193-196.

Khalili, N. & Khabbaz, M.H. 1998. A unique relationship for χ for the determination of the shear strength of unsaturated soils. *Géotechnique* 48(5): 681-687.

Khalili, N., Khabbaz, M.H. & Valliappan, S. 2000. Effective stress based numerical model for hydro-mechanical analysis in unsaturated porous media. *Computational Mechanics* 26(2): 174-184.

Khalili, N., Geiser, F. & Blight, G.E. 2004. Effective stress in unsaturated soils: Review with new evidence. *International Journal of Geomechanics* 4(2): 115-126.

Khalili, N., Habte, M.A. & Zargarbashi, S. 2008. A fully coupled flow deformation model for cyclic analysis of unsaturated soils including hydraulic and mechanical hysteresis. *Computers and Geotechnics* 35(6): 872-889.

Khoshghalb, A. & Khalili, N. 2013. A meshfree method for fully coupled analysis of flow and deformation in unsaturated porous media. *International Journal for Numerical and Analytical Methods in Geomechanics* 37(7): 716-743.

Lenhard, R.J. & Parker, J.C. 1987. A model for hysteretic constitutive relations governing multiphase flow: 2. Permeability-saturation relations. *Water Resources Research* 23(12): 2197-2206.

Lu, N. & Likos, W.J. 2006. Suction stress characteristic curve for unsaturated soil. *Journal of Geotechnical and Geoenvironmental Engineering* 132(2): 131-142.

Mašín, D. 2010. Predicting the dependency of a degree of saturation on void ratio and suction using effective stress principle for unsaturated soils. *International Journal for Numerical and Analytical Methods in Geomechanics* 34(1): 73-90.

Matyas, E.L. & Radhakrishna, H.S. 1968. Volume Change Characteristics of Partially Saturated Soils. *Géotechnique* 18(4): 432-448.

Mualem, Y. 1976. A new model for predicting the hydraulic conductivity of unsaturated porous media. *Water resources research* 12(3): 513-522.

Nuth, M. & Laloui, L. 2008. Advances in modelling hysteretic water retention curve in deformable soils. *Computers and Geotechnics* 35(6): 835-844.

Pasha, A.Y., Khoshghalb, A. & Khalili, N. 2015. Pitfalls in Interpretation of Gravimetric Water Content–Based Soil-Water Characteristic Curve for Deformable Porous Media. *International Journal of Geomechanics* 16(6): D4015004.

Pasha A.Y., Khoshghalb, A. & Khalili, N. 2017. Hysteretic model for the evolution of water retention curve with void ratio. *Journal of Engineering Mechanics*, ASCE 143(7): 04017030.

Romero, E., Della Vecchia, G. & Jommi, C. 2011. An insight into the water retention properties of compacted clayey soils. *Géotechnique* 61(4): 313-328.

Sun, D.A., Cui, H.B., Matsuoka, H. & Sheng, D.C. 2007. A three-dimensional elastoplastic model for unsaturated compacted soils with hydraulic hysteresis. *Soils and Foundations* 47(2): 253-264.

Tarantino, A. 2009. A water retention model for deformable soils. *Géotechnique* 59(9): 751-762.

van Genuchten, M.T. 1980. A closed-form equation for predicting the hydraulic conductivity of unsaturated soils. *Soil Science Society of America Journal* 44(5): 892-898.

Vanapalli, S., Fredlund, D. & Pufahl, D. 1999. The influence of soil structure and stress history on the soil–water characteristics of a compacted till. *Géotechnique* 49(2): 143-159.

Vanapalli, S.K., Fredlund, D.G., Pufahl, D.E. & Clifton, A.W. 1996. Model for the prediction of shear strength with respect to soil suction. *Canadian Geotechnical Journal* 33(3): 379-392.

Vaunat, J., Cante, J., Ledesma, A. & Gens, A. 2000. A stress point algorithm for an elastoplastic model in unsaturated soils. *International Journal of Plasticity* 16(2): 121-141.

Wheeler, S.J., Sharma, R.S. & Buisson, M.S.R. 2003. Coupling of hydraulic hysteresis and stress-strain behaviour in unsaturated soils. *Géotechnique* 53(1): 41-54.

Zhou, A.N., Sheng, D. & Carter, J.P. 2012. Modelling the effect of initial density on soil-water characteristic curves. *Géotechnique* 62(8): 669-680.